
This is an electronic reprint of the original article.
This reprint may differ from the original in pagination and typographic detail.

Author(s): Rackauskas, Simas & Nasibulin, Albert G. & Jiang, Hua & Tian, Ying & Statkute, Gintare & Shandakov, Sergey D. & Lipsanen, Harri & Kauppinen, Esko I.

Title: Mechanistic investigation of ZnO nanowire growth

Year: 2009

Version: Final published version

Please cite the original version:

Rackauskas, Simas & Nasibulin, Albert G. & Jiang, Hua & Tian, Ying & Statkute, Gintare & Shandakov, Sergey D. & Lipsanen, Harri & Kauppinen, Esko I. 2009. Mechanistic investigation of ZnO nanowire growth. Applied Physics Letters. Volume 95, Issue 18. P. 183114/1-3. ISSN 0003-6951 (printed). DOI: 10.1063/1.3258074.

Rights: © 2009 American Institute of Physics. This article may be downloaded for personal use only. Any other use requires prior permission of the author and the American Institute of Physics.
<http://scitation.aip.org/content/aip/journal/jap>

All material supplied via Aaltodoc is protected by copyright and other intellectual property rights, and duplication or sale of all or part of any of the repository collections is not permitted, except that material may be duplicated by you for your research use or educational purposes in electronic or print form. You must obtain permission for any other use. Electronic or print copies may not be offered, whether for sale or otherwise to anyone who is not an authorised user.

Mechanistic investigation of ZnO nanowire growth

Simas Rackauskas, Albert G. Nasibulin, Hua Jiang, Ying Tian, Gintare Statkute, Sergey D. Shandakov, Harri Lipsanen, and Esko I. Kauppinen

Citation: *Applied Physics Letters* **95**, 183114 (2009); doi: 10.1063/1.3258074

View online: <http://dx.doi.org/10.1063/1.3258074>

View Table of Contents: <http://scitation.aip.org/content/aip/journal/apl/95/18?ver=pdfcov>

Published by the [AIP Publishing](#)

Articles you may be interested in

Defects in ZnO

J. Appl. Phys. **106**, 071101 (2009); 10.1063/1.3216464

Effect of high-energy electron beam irradiation on the properties of ZnO thin films prepared by magnetron sputtering

J. Appl. Phys. **105**, 123509 (2009); 10.1063/1.3149783

A comparative analysis of deep level emission in ZnO layers deposited by various methods

J. Appl. Phys. **105**, 013502 (2009); 10.1063/1.3054175

Secondary growth of small ZnO tripodlike arms on the end of nanowires

Appl. Phys. Lett. **91**, 013106 (2007); 10.1063/1.2752605

Femtosecond laser assisted growth of ZnO nanowires

Appl. Phys. Lett. **87**, 133115 (2005); 10.1063/1.2061858

An advertisement for Oxford Instruments' Atomic Force Microscope (AFM). The background is dark blue with a lighter blue gradient. On the left, there is a black mobile phone and a beige desktop computer. In the center, there is a white AFM instrument. Text on the left side reads: 'You don't still use this cell phone or this computer'. Text in the center reads: 'Why are you still using an AFM designed in the 80's?'. Text on the right side reads: 'It is time to upgrade your AFM', 'Minimum \$20,000 trade-in discount for purchases before August 31st', and 'Asylum Research is today's technology leader in AFM'. At the bottom right, there is the Oxford Instruments logo and the tagline 'The Business of Science®'. The email address 'dropmyoldAFM@oxinst.com' is also present.

Mechanistic investigation of ZnO nanowire growth

Simas Rackauskas,^{1,a)} Albert G. Nasibulin,^{1,a)} Hua Jiang,¹ Ying Tian,¹ Gintare Statkute,² Sergey D. Shandakov,³ Harri Lipsanen,² and Esko I. Kauppinen^{1,4}

¹Department of Applied Physics and Center for New Materials, NanoMaterials Group, Helsinki University of Technology, P.O. Box 5100, 02015 Espoo, Finland

²Department of Micro and Nanosciences, Micronova, Helsinki University of Technology, 02015 Espoo, Finland

³Department of Physics, Laboratory of Carbon NanoMaterials, Kemerovo State University, Kemerovo 650043, Russia

⁴VTT Biotechnology, Biologinkuja 7, 02044 Espoo, Finland

(Received 5 August 2009; accepted 12 October 2009; published online 6 November 2009)

ZnO nanowire (NW) growth mechanism was investigated in a nonvapor and noncatalytic approach for the controlled NW synthesis in a second time scale. The experimental results showed that ZnO NW growth was determined by migration of zinc interstitials and vacancies in a ZnO layer, which should be also considered in other synthesis techniques and mechanisms. The mechanism of the ZnO NW growth was explained as due to the advantageous diffusion through grain boundaries in ZnO layer and crystal defects in NWs. Additionally, on the basis of photoluminescence measurements, a feasible application of as-produced wires for optoelectronic devices was demonstrated. © 2009 American Institute of Physics. [doi:10.1063/1.3258074]

Nanostructured ZnO materials have received broad attention due to their distinguished performance in electronics, optics, and photonics.¹ In particular, ZnO nanowires (NWs) are regarded as promising candidates for optoelectronic applications such as room temperature UV laser diodes due to their wide band gap energy of 3.37 eV and high exciton binding energy of about 60 meV.^{2,3} Common ZnO NW synthesis methods include metal-organic chemical vapor deposition,⁴ vapor synthesis,⁵ hydrothermal,^{6,7} and chemical solution route.⁸ Typically, the NW growth has been explained by vapor-liquid-solid⁹ or vapor-solid¹⁰ mechanisms.

Here, we synthesized ZnO NWs and investigated the growth mechanism on the basis of proposed synthesis method.^{11,12} High crystallinity ZnO NWs are produced without catalyst and dominant role of Zn and ZnO vapors, in a second time scale. Based on experimental results we show that ZnO NW growth is determined by zinc interstitial migration in a ZnO layer. This growth mechanism should be also considered in other synthesis techniques.^{13,14} Additionally, on the basis of photoluminescence (PL) measurements, we demonstrated feasible application of the as-produced NWs for optoelectronic devices.

The detailed description of the ZnO NW synthesis method is given elsewhere.¹¹ ZnO NW synthesis was carried out by resistive heating of a Zn wire under ambient air conditions in the range of 673–1123 K, i.e., at temperatures near or higher than the melting point of zinc (692 K). During the synthesis a protective 0.5–1 μm thickness of ZnO layer forms on the surface of Zn wire [Fig. 1(a)], which preserves the shape of the liquefied wire. ZnO NWs grow on the surface of the ZnO layer and have typical diameters in the range of 6–30 nm and lengths between 1 and 5 μm . At specific conditions, when Zn wire is heated too quickly, the ZnO layer breaks, and the NWs can grow up to 40 μm , by vapor growth mechanism [Fig. 1(b)]. In order to avoid this, synthe-

sis conditions were reached by gradually heating zinc wire and carefully controlling the temperature by an IR pyrometer.

Transmission (TEM) and scanning (SEM) electron microscopic studies were performed. Figures 1(c) and 1(d) show the results of TEM investigations of the structures of the ZnO NWs grown at 803 K. Importantly, ZnO NWs synthesized at higher temperatures had fewer defects, while low temperature samples usually contained stacking faults [Fig. 1(c)]. An inset of Fig. 1(c) is an electron diffraction pattern revealing extra weak spots resulting from the stacking faults that periodically appear along $[1\bar{1}0]$ direction. Figure 1(d) shows a crystalline ZnO NW without stacking faults, as de-

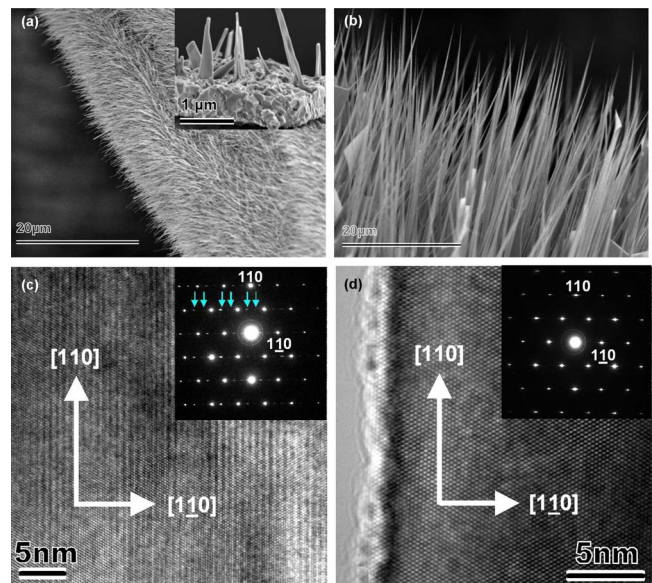


FIG. 1. (Color online) Electron microscopic studies of ZnO NWs: SEM image of (a) typical ZnO NW forest (inset shows ZnO layer formed on the surface of Zn wire at 1023 K) and (b) NWs up to 40 μm long. [(c) and (d)] High resolution TEM images of ZnO NWs, insets are corresponding electron diffraction patterns.

^{a)}Authors to whom correspondence should be addressed. Electronic addresses: simas.rackauskas@tkk.fi and albert.nasibulin@tkk.fi.

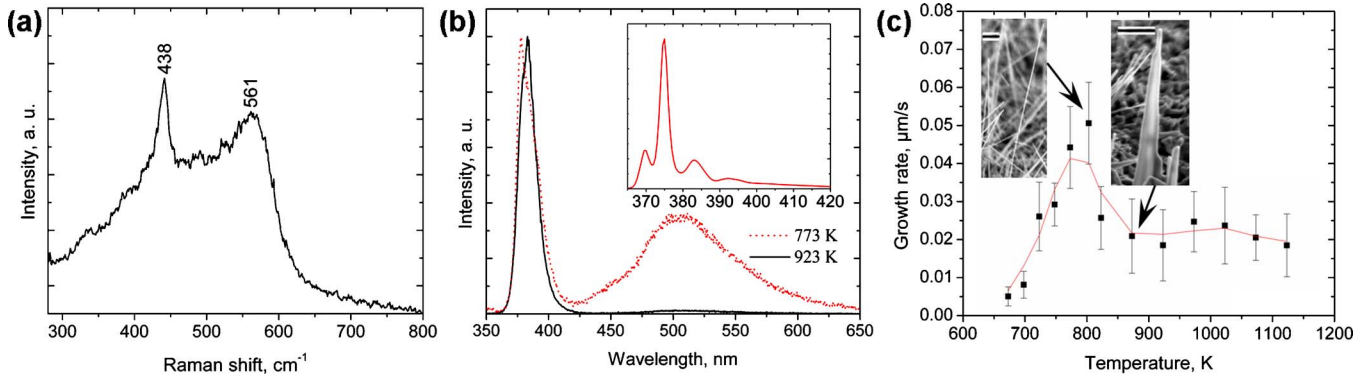


FIG. 2. (Color online) (a) Raman spectrum of ZnO NWs grown at 773 K; (b) Room temperature PL spectra of ZnO nanowires. Inset shows low temperature PL spectrum of ZnO NWs grown at 773 K; (c) growth rate dependence on the process temperature and SEM images of ZnO NWs at indicated temperatures (scale bar 500 nm).

terminated by rotation of the NW in TEM. The electron diffraction pattern from the ZnO NW was indexed as hexagonal ZnO lattice structure with the crystallographic parameters of $a=0.325$ and $c=0.521$ nm. In all cases the growth direction of the ZnO NW was determined to be [110].

Chemical composition of the wire surface after the synthesis was examined by Raman spectroscopy measurements [Fig. 2(a)], using Wintech alpha300 spectrometer ($\lambda=532$ nm power 160 μ W). The peak centered at 438 cm^{-1} corresponds to E2 mode of ZnO and the peak at 561 cm^{-1} is related to the oxygen deficiency in ZnO.^{15,16}

Room temperature PL measurements were made using a He–Cd laser ($\lambda=325$ nm, power 10 mW). PL spectra [Fig. 2(b)] of the ZnO NW samples reveal two peaks with a variable intensity. One peak, referred to as the excitonic emission or band gap emission, is located around 380 nm. The other deep trap emission peak in the visible region, centered at 510 nm, is due to impurities or defects, which have electronic energy levels within the band gap of ZnO.^{17,18} Typically, both peaks are present in the synthesis temperature range of 723–923 K (Fig. 2). In samples grown at higher process temperature (923–1023 K), the band gap emission dominates. This can be attributed to higher crystallinity and lower amount of defects at higher temperatures.

Low temperature PL measurements (Fig. 2 inset) at 10K (laser $\lambda=266$ nm, 2nd harmonics power 6 W) showed emission in UV region consisting of up to four peaks, which were considered to originate from excitons, acceptor-exciton complexes, and phonon replicas.¹⁹ The dominating bound exciton

peak is located at 375 nm, free exciton emission peak is observed at 368 nm. Other peaks on the lower energy side, can be attributed to phonon replicas of either donor or acceptor bound excitons.¹⁹

In order to investigate the kinetics of the NW growth, we prepared samples at different temperatures with a fixed growth time of 1 min. The lengths of the NWs obtained from SEM images were used for the calculations of the average growth rate [Fig. 2(c)]. Two regions can be clearly distinguished in this plot: kinetic and constant growth rate. In the kinetic region, the average NW growth rate increases with the temperature rise until 803 K. At higher temperatures NW growth rate remains nearly constant. It is worth noting that the surface density of the NWs significantly decreases at higher temperatures. ZnO NW shape also undergoes a change from rodlike (at temperatures ≤ 803 K) to swordlike shape at temperatures above 850 K.

Also, we examined the kinetics of ZnO NW growth at the fixed temperature of 803 K, where the growth rate is the highest. It is known that during Zn oxidation ZnO layer thickens according to the parabolic law,^{20,21} which is associated with diffusion of Zn vacancies and interstitials.²² The vacancy and interstitial migration rate r_m can be expressed as

$$r_m = A\tau^{-0.5}, \quad (1)$$

where A is a coefficient of proportionality, τ is time. Plotting the kinetic data of the ZnO NW growth rate r_g at 803 K in the coordinates $\ln r_g - \ln \tau$ gives a similar linear dependence [Fig. 3(a)],

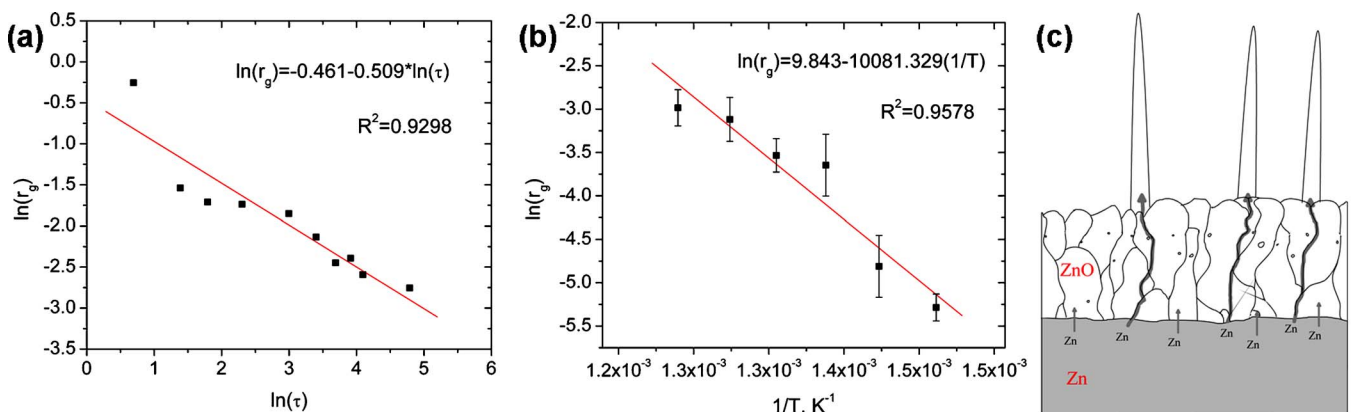


FIG. 3. (Color online) Kinetic data of ZnO NW growth: (a) growth rate ($\mu\text{m/s}$) dependence on time (s) in a double logarithmic scale; (b) kinetic region (673–803 K) data of the growth rate in the Arrhenius coordinates; (c) schematics of ZnO NW growth mechanism.

$$\ln r_g = -0.4721 - 0.5095 \ln \tau. \quad (2)$$

Consequently it can be concluded that the NW growth rate r_g has also parabolic time dependence. This indicates that ZnO NW growth is determined by migration of Zn vacancies or interstitials.

The rate of ZnO NW growth can be expressed by Arrhenius dependence,

$$r_g = \frac{dL}{dt} = k_0 \exp\left(-\frac{E_a}{RT}\right), \quad (3)$$

where L is the length of NW, k_0 is the pre-exponential coefficient, E_a is the activation energy of the NW growth, R is the gas constant, and T is the absolute temperature. Furthermore, plotting the kinetic region (673–803 K) data of the growth rate in the Arrhenius coordinates $\ln r_g - 1/T$ gives a linear dependence [Fig. 3(b)], from which the activation energy was found to be $E_a = 83.8$ kJ/mol. This value can be attributed to the migration energy of Zn interstitials and vacancies (77 and 88 kJ/mol, respectively).²³ Migration of oxygen interstitials is less probable because of larger oxygen size. Indeed, oxygen interstitial and vacancy migration energies are 118 and 124 kJ/mol, respectively.²³ The activation energy for ZnO lattice diffusion is as high as 305 kJ/mol^{20,22} and, as a result, cannot be attributed to the limiting stage of the NW growth. Therefore, it can be deduced that the growth of ZnO NWs complies with the parabolic law and determined by zinc interstitial and vacancy migration.

Based on the oxidation mechanism and our investigations, ZnO NW growth mechanism can be proposed. According to the metal oxidation mechanism^{20,23,24} zinc oxidation involves Zn diffusion from Zn–ZnO interface to the surface [Fig. 3(c)]. Advantageous diffusion through grain boundaries comparing to lattice diffusion^{20,23} creates sites on the surface, from which ZnO NWs grow. Rodlike shape of ZnO NW is created through anisotropic Zn diffusion in the direction of energetically favorable crystal growth [110]. The optimum growth conditions for dense ZnO NW “forest” occur at 803 K. At temperatures ≥ 850 K, the size of ZnO grains becomes larger,²⁵ so that there is less grain boundary space for rapid diffusion to occur. This is confirmed from SEM images as density of ZnO NW on the surface at temperatures above 803 K is lower.

The growth of the NWs is also determined by the presence of defects such as stacking faults. The amount of the synthesized NWs was drastically decreased when the temperature was above 803 K, which is likely explained by the formation of the NWs with higher crystallinity. TEM and PL investigations confirmed the presence of fewer defects and less surface NW density at higher synthesis temperatures. However, the annealing of ZnO NWs at high temperatures should not be neglected, since NWs appear on the surface already after 10 s.

To conclude, ZnO NW growth mechanism was investigated in a NW growth method based on resistive heating in the temperature range of 673–1123 K. The highest ZnO NW growth rate was observed at 803 K. It was found that the

direction of the ZnO NWs occurs along [110]. The growth rate had parabolic dependence, which was explained by Zn interstitial and vacancy migration. ZnO NW growth activation energy $E_a = 83.8$ kJ/mol, obtained from the Arrhenius plot, confirmed this result. Zinc interstitial and vacancy migration were deduced to be the limiting stage of the ZnO NWs growth. The mechanism of the ZnO NW growth was explained as due to the advantageous diffusion through grain boundaries in ZnO layer and crystal defects in NWs. Room temperature PL spectra show band gap emission located around 380 nm and deep trap emission peak centered at 510 nm. High synthesis temperature ZnO NWs show lower intensity of deep emission, which confirms higher NW crystallinity. Low temperature PL spectrum shows peaks, originating from excitons, acceptor-exciton complexes and phonon replicas.

This work was supported by the Academy of Finland (Project Nos. 128445, 124283, and 128495).

¹Z. L. Wang, *Mater. Sci. Eng., R.* **64**, 33 (2009).

²Z. L. Wang, *J. Phys.: Condens. Matter* **16**, R829 (2004).

³M. H. Huang, S. Mao, H. Feick, H. Q. Yan, Y. Y. Wu, H. Kind, E. Weber, R. Russo, and P. D. Yang, *Science* **292**, 1897 (2001).

⁴W. I. Park, D. H. Kim, S. W. Jung, and G. C. Yi, *Appl. Phys. Lett.* **80**, 4232 (2002).

⁵Z. R. Dai, Z. W. Pan, and Z. L. Wang, *Adv. Funct. Mater.* **13**, 9 (2003).

⁶K. Elen, H. Van den Rul, A. Hardy, M. K. Van Bael, J. D’Haen, R. Peeters, D. Franco, and J. Mullens, *Nanotechnology* **20**, 055608 (2009).

⁷J. Wang and L. Gao, *Solid State Commun.* **132**, 269 (2004).

⁸H. Zhang, X. Y. Ma, J. Xu, J. J. Niu, and D. R. Yang, *Nanotechnology* **14**, 423 (2003).

⁹R. S. Wagner and W. C. Ellis, *Appl. Phys. Lett.* **4**, 89 (1964).

¹⁰Z. W. Pan, Z. R. Dai, and Z. L. Wang, *Science* **291**, 1947 (2001).

¹¹S. Rackauskas, A. G. Nasibulin, H. Jiang, Y. Tian, V. I. Kleshch, J. Sainio, E. D. Obraztsova, S. N. Bokova, A. N. Obraztsov, and E. I. Kauppinen, *Nanotechnology* **20**, 165603 (2009).

¹²A. Nasibulin, S. Rackauskas, H. Jiang, Y. Tian, P. Mudimela, S. Shandakov, L. Nasibulina, S. Jani, and E. Kauppinen, *Nano Res.* **2**, 373 (2009).

¹³Z. Gu, M. P. Paranthaman, J. Xu, and Z. W. Pan, *ACS Nano* **3**, 273 (2009).

¹⁴N. Boukos, C. Chandrinou, K. Giannakopoulos, G. Pistoris, and A. Travlos, *Appl. Phys. A: Mater. Sci. Process.* **88**, 35 (2007).

¹⁵X. Wang, Q. Q. Li, Z. B. Liu, J. Zhang, Z. F. Liu, and R. M. Wang, *Appl. Phys. Lett.* **84**, 4941 (2004).

¹⁶H. Pan, Y. W. Zhu, Z. H. Ni, H. Sun, C. Poh, S. H. Lim, C. Sow, Z. X. Shen, Y. P. Feng, and J. Y. Lin, *J. Nanosci. Nanotechnol.* **5**, 1683 (2005).

¹⁷A. F. Kohan, G. Ceder, D. Morgan, and C. G. Van de Walle, *Phys. Rev. B* **61**, 15019 (2000).

¹⁸S. Eustis, L. H. Robins, and B. Nikoobakht, *J. Phys. Chem. C* **113**, 2277 (2009).

¹⁹H. Zhou, M. Wissinger, J. Fallert, R. Hauschild, F. Stelzl, C. Klingshirn, and H. Kalt, *Appl. Phys. Lett.* **91**, 181112 (2007).

²⁰D. Young, *High Temperature Oxidation and Corrosion of Metals* (Elsevier, Oxford, 2008), Vol. 1, p. 592.

²¹I. E. Geguzin, *Diffusion Zone [in Russian]* (Nauka, Moscow, 1979), p. 344.

²²W. W. Smeltzer and D. J. Young, *Prog. Solid State Chem.* **10**, 17 (1975).

²³G. W. Tomlins, J. L. Routbort, and T. O. Mason, *J. Appl. Phys.* **87**, 117 (2000).

²⁴C. Wagner, *Prog. Solid State Chem.* **10**, 3 (1975).

²⁵K. K. Khristoforov, B. K. Avdeenko, I. G. Portnova, Y. A. Omel’chenko, and A. V. Chernykh, *Glass Ceram.* **43**, 171 (1986).